Expansion of Renewable Energy Capacities in Microgrids Using Robust Control Approaches

Van Tan Nguyen[1,*], Huu Hieu Nguyen[1], Kim Hung Le[1], and The Khanh Truong[1]

ARTICLE INFO

Article history:
Received: 16 June 2020
Revised: 12 August 2020
Accepted: 20 August 2020

Keywords:
Microgrids
Renewable energy sources
Robust control
H-infinity control
Energy storage

ABSTRACT

With the endless growth of renewable energy sources recently, the integration of these sources into factories, public infrastructures (airports, train stations, hospitals, etc.) forming microgrid systems is becoming a trend in the evolution of modern power systems. However, the increasing participation and expansion of renewable energy sources into the power system still faces many challenges due to the instability, oscillation and unpredictability of these type of generators. In order to ensure the quality criteria of a standard grid (frequency stability, voltage stability, ...), this paper proposes a H-infinity robust control method for the purpose of controlling distributed generators in microgrids, particularly energy storage systems, because this approach is suitable for controlling objects with various uncertainties. Then, the analysis and evaluation are given through simulation results with different penetration levels of renewable energy sources using Matlab/Simulink software, thereby emphasizing the role of the H-infinity robust controller in microgrids with the expansion of renewable energy.

1. INTRODUCTION

Microgrid, a popular concept that appeared in previous studies of power system technology, is now becoming an inevitable trend in the electricity industry in the context of the continuous development of generators in general and renewable energy sources in particular. Microgrid was created to overcome global energy challenges, to meet the demand of power consumption, power quality and environmental issues worldwide. In the Microgrid structure, the power sources are located close to the power consumers so it brings us many advantages such as reducing transmission losses, reducing requirements on transmission and distribution infrastructure, increasing reliability, reducing emissions, improving power quality and reducing electricity costs. Specially, the rise of renewable energy sources in the power system has brought not only benefits but also negative impacts to providers as well as consumers when penetrating to existing power systems.

The concept of Microgrid has been defined and mentioned in many studies [1]-[3]. In general, Microgrid is a small-scale power grid consisting of distributed generators (DG) combined with energy storage systems (ESS) that provide electricity to loads (industry, household, lighting, ...). DG and ESS in Microgrid include dispatchable and non-dispatchable units. Dispatchable units are generation units which can adjust their power to the reference value and respond to disturbance changes during operation. Non-dispatchable units are those with their power dependent on external factors (weather, physical nature, ...) and cannot be controlled to the preset values. Thus, non-dispatchable units always delivery maximum capacity to fully exploit its potential.

Most of renewable energy sources are non-dispatchable units, so high proportion of renewables in the power system is the main cause of power fluctuation as well as poor dynamic stability. Especially, when Microgrid operates in islanded mode, there are no support or auxiliary solutions from the utility grid to maintain the stability of the Microgrid. As a result, the ESS with their high-power exchange density can be the key of power balance and dynamic stability in Microgrid against the uncertainty of renewables. Compared to large-scale power systems, islanded Microgrid has low system inertia due to the high integration of renewable energy sources and ESS. Therefore, this paper aims to find an approach to increase the penetration rate of renewable energy sources while achieving multiple objectives such as ensuring frequency and voltage stability, improving power quality and adaptive controller design to ensure power balance in the system with uncertain factors [4].

[1]*Faculty of Electrical Engineering, The University of Danang – University of Science and Technology, 54 Nguyen Luong Bang St., Da Nang city, Vietnam.*

**Corresponding author:* Van Tan Nguyen; E-mail: tan78dhbk@dut.udn.vn.

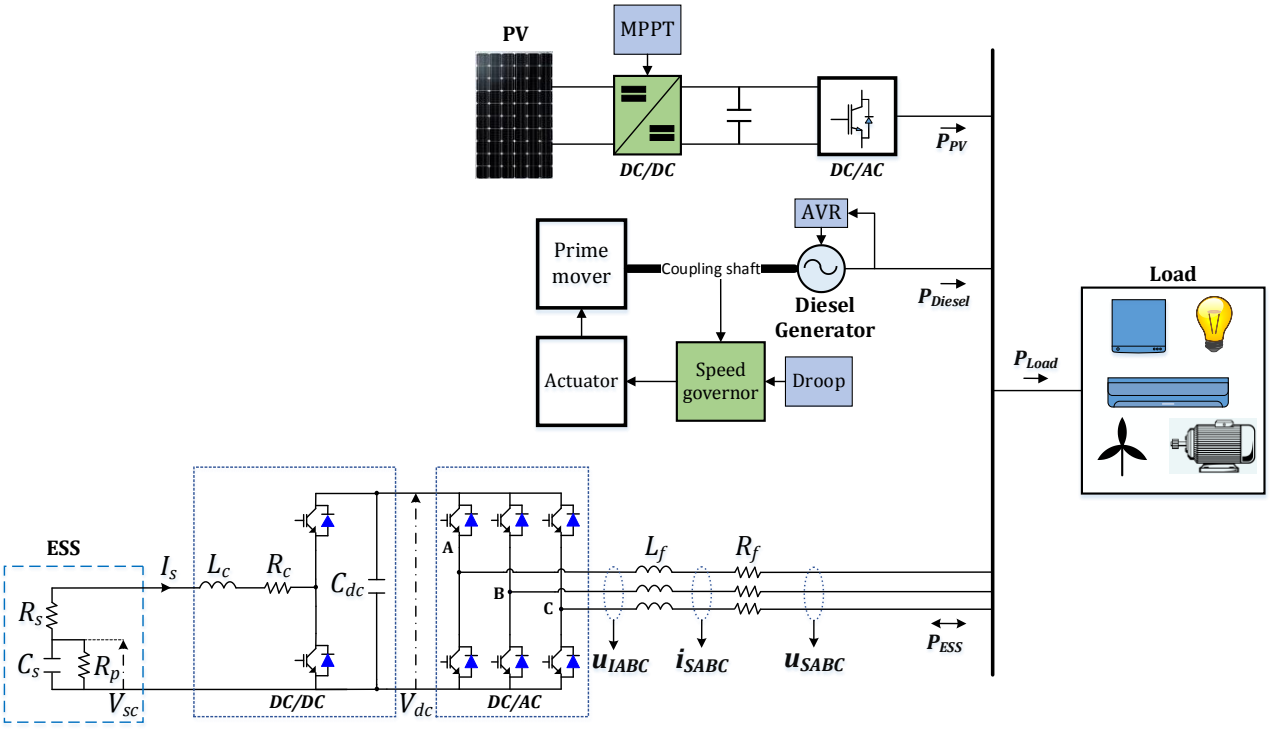

Fig. 1: Studied model of the Microgrid system.

In [5], [6], the basic and simplest control method for islanded Microgrid has been presented, which is called droop control method. However, the traditional droop method in primary frequency control still has many limitations such as low response rate, trade-off between voltage regulation and load sharing and difficulties in integrating renewable energy sources [7]. In addition, some studies on the application of the H-infinity robust control algorithm in Microgrid were also illustrated in [8]–[12], but only in terms of power quality (voltage, frequency), uncertainty factors in the Microgrid system without mentioning the penetration rate of renewable energy sources in the system. This paper proposes a H-infinity control approach integrated into the ESS of Microgrid in islanded mode and then consider different penetration levels of renewable energy sources (namely photovoltaic solar power) to assess the stability of the system with the expansion of renewable energy sources, thereby leading to the construction and development of power systems using entirely renewable energy sources.

2. SYSTEM DESIGN

2.1 Studied system model

During the study, authors focused on controlling the energy storage system to ensure power sharing in islanded mode (or off-grid mode). Therefore, the units in the system are selected and modeled in accordance with this operating mode. To meet the goal of power balance and transient stability when operating in islanded mode, the studied system is shown in Fig. 1, including a diesel generator (using Automatic Voltage Regulator - AVR), a photovoltaic system and a storage system.

2.2 Unit modelling

As mentioned above, the studied system model is provided for the control of the storage system, so other units (Load, Diesel, PV) will act as a disturbance signal of the system. More specifically, the modelling from the storage system to the AC bus will include the storage system (characterized by capacitance C_s, serial resistance R_s and parallel resistance R_p), DC/DC bidirectional converter (characterized by inductance L_c and resistance R_c of the coil, capacitance C_{dc} at DC bus and two power electronic valves), DC/AC converter and filter coil (characterized by inductance L_f and resistance R_f).

In the studied model, the PV system is frequently fluctuated due to many factors (weather changes, shading phenomenon, ...), leading to large power fluctuations. In Fig. 1, the PV system is integrated with the maximum power point tracking (MPPT) algorithm to maximize the generation capacity of the solar source and minimize the power burden on other sources. Modelling of PV system with MPPT algorithm has been proposed, studied and analyzed in [13]–[15], so the PV model is simply shown in Fig. 1, the PV system is integrated with the maximum power point tracking (MPPT) algorithm to maximize the generation capacity of the solar source and minimize the power burden on other sources. Modelling of PV system with MPPT algorithm has been proposed, studied, and analyzed in [13]-[15], so the PV model is simply shown in

Fig. 1.

Diesel generator model in Fig. 1 includes speed governor controlled by droop method, diesel engine and other transmission parts (actuator, coupling shaft). In addition, the diesel generator uses the AVR to ensure the terminal voltage remains stable during operation. The transmission stages in the diesel generator are characterized by a time constant T_{diesel} and the droop control stage is characterized by the droop coefficient s_{diesel}, shown in Fig. 2.

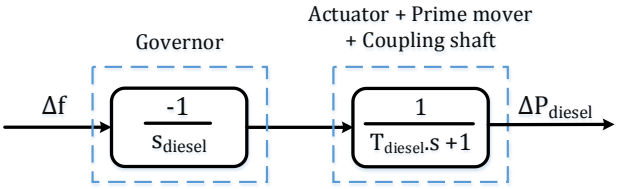

Fig. 2. Dynamic model of diesel generator.

2.3 Microgrid dynamic model

In the operation of the Microgrid, to ensure system frequency stability, the power balance between the sources and the load should be maintained. In the dynamic model of the system is presented in Figure 3. According to that, the system is characterized by two constants H (system inertia constant) and D (load damping) [16]. Assuming that the power values are noise values, the dynamic model of Microgrid is derived as (1):

$$\frac{d\Delta f}{dt} = \frac{1}{2H}\left[\left(\Delta P_{PV} + \Delta P_{diesel} + \Delta P_{ESS} - \Delta P_{load}\right) - D\Delta f\right] \quad (1)$$

where: Δf is the frequency deviation of the system, $\Delta P_{PV}, \Delta P_{diesel}, \Delta P_{ESS}, \Delta P_{load}$ are respectively the active power difference of PV system, diesel generator, ESS and load.

Applying Laplace transform to (1), the dynamic equation of the Microgrid is obtained as follow:

$$\Delta f(s) = \frac{1}{2H + D}\left[\Delta P_{PV}(s) + \Delta P_{diesel}(s) + \Delta P_{ESS}(s) - \Delta P_{load}(s)\right] \quad (2)$$

3. H-INFINITY ROBUST CONTROL

In this section, an overview of the robust control theory applied in the paper will be demonstrated. The advantage of a robust control system is that the quality of the control objects in the system is always kept stable according to the pre-set criteria, regardless of the change of system parameters as well as the disturbance value on the system. Furthermore, the robust controller is optimized for multi-input multi-output (MIMO) systems, so is suitable for applying to the studied model.

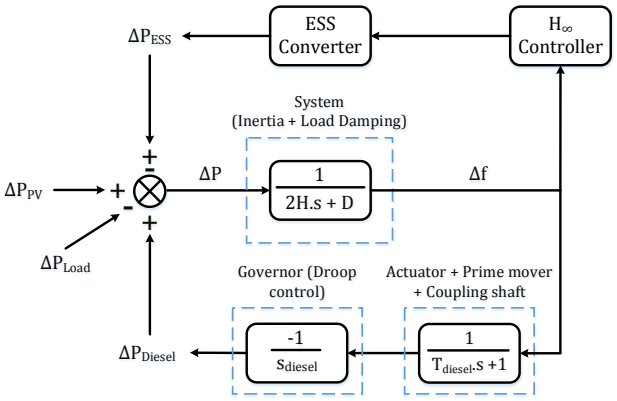

Fig. 3. Dynamic model of studied Microgrid system.

Based on the classical closed-loop feedback control problem shown in Fig. 4, the general control structure of the robust control system is given in Fig. 5, also known as the P-K control structure. Robust control using P-K structure based on mixed-sensitivity problem, that is, finding suitable weighting functions for error signal z that satisfy the performance conditions in order to synthesize the controller K [17].

From Fig. 5:

$$z = N.w \quad (3)$$

where: $N = \begin{bmatrix} W_v S \\ W_u KS \end{bmatrix}$ is the transfer function from z to w, S is the sensitivity function, W_u and W_v are the performance weighting functions of input and output signal of controller K respectively [17].

The problem is minimizing the value of the error signal z, that is, to find the minimum of the infinity norm of the transfer function N, denoted by $\min_K \left\|N(K)\right\|_\infty$.

The weighting functions for control input signal v and control output signal u of controller K are based on the transfer function of first-order filter (which is called the performance weight) that is given in [17]:

$$W(s) = \frac{s/M + \omega_B^*}{s + \omega_B^* A} \quad (4)$$

where, A is the maximum steady-state tracking error, M is the maximum peak magnitude of S, ω_B^* is the minimum bandwidth frequency (defined as the frequency where $|S(j\omega)|$ crosses 0.707 from below). Typically, we select $M = 2$, $A \approx 1$[17].

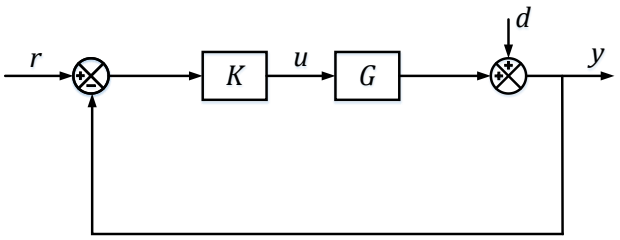

Fig. 4. Block diagram of classical closed-loop feedback control.

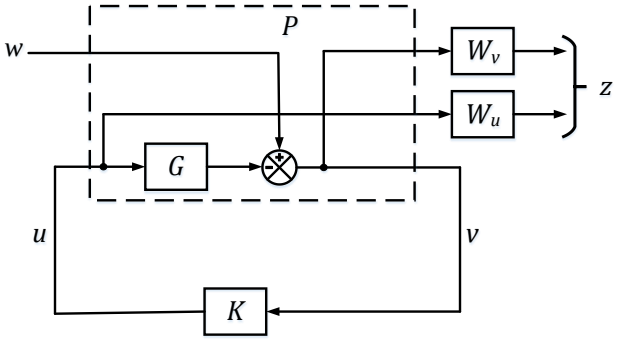

Fig. 5. Block diagram of P-K structure robust control.

4. APPLICATION OF ROBUST CONTROL IN STUDIED SYSTEM

In this section, the author will provide the steps to apply the H-infinity algorithm for analyzing the primary frequency stability with the expansion of PV power. The control object is defined as the ESS and control signals are modulation indices of DC/DC bidirectional converter and DC/AC converter. As such, the controller is designed to have one input (system frequency) and multiple outputs (modulation indices). The proposed control scheme is shown in Fig. 6. Accordingly, three-phase values will be converted to dq-frame values to reduce complexity in the calculation equations.

In summary, the process of applying robust control algorithm to the system is given as follows:

- Building state-space model of the control object through derivative equations derived from the modelling of generation units.
- Selecting weighting functions for controller input and output signals.
- Computing controllers using calculation toolbox from Matlab/Simulink software.
- Simulation of the Microgrid with different penetration rates of PV source when using robust controller.

4.1 Building state-space model

Building the state-space model of the ESS will be based on the equivalent circuit modelling shown in Fig. 6. Considering the averaged small-signal model, related equations are derived as follows [16], [18]:

$$\frac{d\Delta V_{sc}}{dt} = -\frac{1}{C_s}\Delta I_s - \frac{1}{R_p C_s}\Delta V_{sc} \quad (5)$$

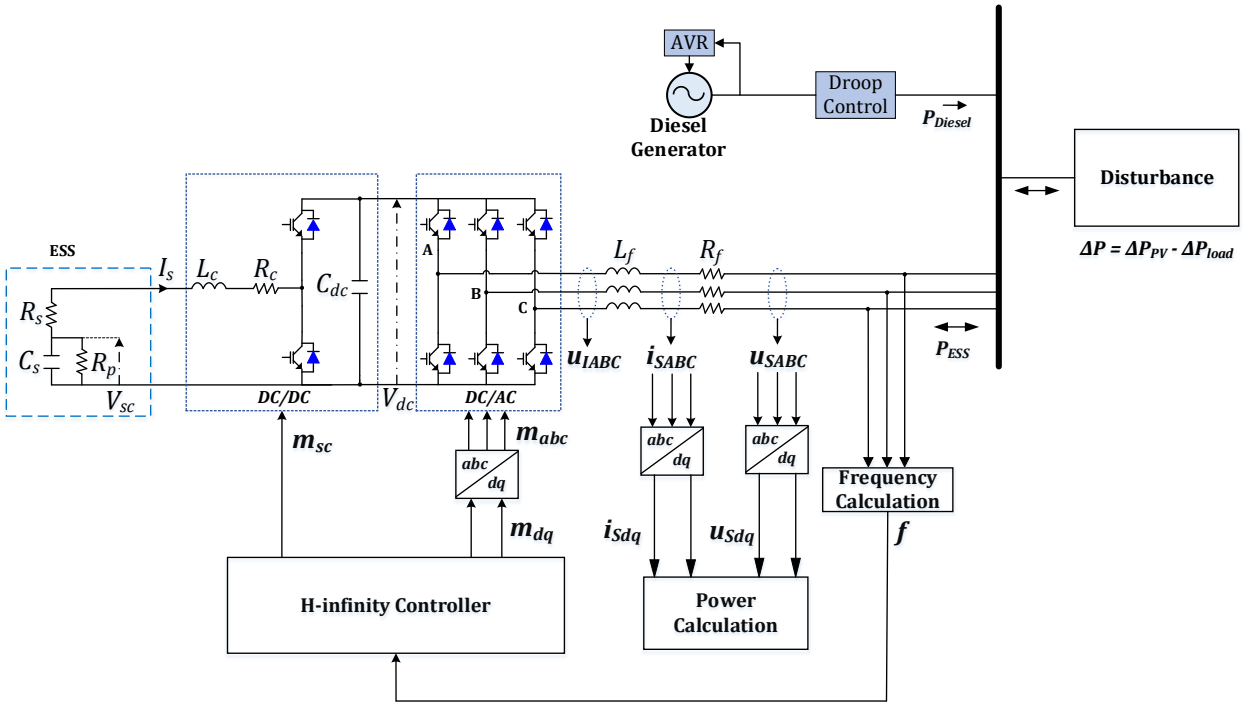

Fig. 6. Proposed Robust H-infinity control scheme.

$$\frac{d\Delta I_s}{dt} = \frac{1}{L_c}\Delta V_{sc} - \frac{R_s + R_c}{L_c}\Delta I_s - \frac{m_{sc_e}}{L_c}\Delta V_{dc} - \frac{V_{dc_e}}{L_c}\Delta m_{sc} \quad (6)$$

$$\frac{d\Delta V_{dc}}{dt} = \frac{m_{sc_e}}{C_{dc}}\Delta I_s + \frac{I_{s_e}}{C_{dc}}\Delta m_{sc} - \frac{1}{C_{dc}}(m_{d_e}\Delta I_{sd} + m_{q_e}\Delta I_{sq} + I_{sd_e}\Delta m_d + I_{sq_e}\Delta m_q) - \frac{1}{R_{dc}C_{dc}}\Delta V_{dc} \quad (7)$$

$$\frac{d\Delta I_{sd}}{dt} = \frac{m_{d_e}}{L_f}\Delta V_{dc} + \frac{V_{dc_e}}{L_f}\Delta m_d - \frac{R_f}{L_f}\Delta I_{sd} + 2\pi f_e \Delta I_{sq} + I_{sq_e} 2\pi\Delta f \quad (8)$$

$$\frac{d\Delta I_{sq}}{dt} = \frac{m_{q_e}}{L_f}\Delta V_{dc} + \frac{V_{dc_e}}{L_f}\Delta m_q - \frac{R_f}{L_f}\Delta I_{sq} + 2\pi f_e \Delta I_{sd} + I_{sd_e} 2\pi\Delta f \quad (9)$$

From the dynamic equations in Section 2, equivalent equations of the diesel generator with droop control and Microgrid system are given:

$$\frac{d\Delta P_{diesel}}{dt} = -\frac{1}{T_{diesel}}\Delta P_{diesel} - \frac{1}{T_{diesel}s_{diesel}}\Delta f \quad (10)$$

$$\frac{d\Delta f}{dt} = \frac{1}{2H}\left[\left(V_{sc_e} - 2R_s I_{s_e}\right)\Delta I_s + I_{s_e}\Delta V_{sc} + \Delta P_{diesel} + \Delta P_{PV} - \Delta P_{load}\right] - \frac{D}{2H}\Delta f \quad (11)$$

In these above equations, units with subscript "e" represent the value at the equilibrium point.

From the averaged small-signal model of storage system, diesel generator and Microgrid, equation (5) to (11) could be combined to build the state-space model with the following general form as follows:

$$\begin{cases} \Delta\dot{x} = A\Delta x + B_1\Delta u + B_2\Delta w \\ \Delta y = C\Delta x + D_1\Delta u + D_2\Delta w \end{cases} \quad (12)$$

where:

$\Delta x = \left[\Delta V_{sc} \;\; \Delta I_s \;\; \Delta V_{dc} \;\; \Delta I_{sd} \;\; \Delta I_{sq} \;\; \Delta P_{diesel} \;\; \Delta f\right]^T$ is the input state vector.

$\Delta u = \left[\Delta m_{sc} \;\; \Delta m_d \;\; \Delta m_q\right]^T$ is the control signal vector (output of the controller).

$\Delta w = \Delta P_{PV} - \Delta P_{load}$ is the input disturbance vector.

$\Delta y = \Delta f$ is the output signal vector (input of the controller).

As a result, state-space matrices A, B_1, B_2, C, D_1, D_2 are obtained in Fig. 7.

$$A = \begin{bmatrix} -\frac{1}{R_p C_s} & -\frac{1}{C_s} & 0 & 0 & 0 & 0 & 0 \\ \frac{1}{L_c} & -\frac{R_s + R_c}{L_c} & -\frac{m_{sc_e}}{L_c} & 0 & 0 & 0 & 0 \\ 0 & \frac{m_{sc_e}}{C_{dc}} & -\frac{1}{R_{dc}C_{dc}} & -\frac{m_{d_e}}{C_{dc}} & -\frac{m_{q_e}}{C_{dc}} & 0 & 0 \\ 0 & 0 & \frac{m_{d_e}}{L_f} & -\frac{R_f}{L_f} & 2\pi f_e & 0 & -2\pi I_{sq_e} \\ 0 & 0 & \frac{m_{q_e}}{L_f} & 2\pi f_e & -\frac{R_f}{L_f} & 0 & -2\pi I_{sd_e} \\ 0 & 0 & 0 & 0 & 0 & -\frac{1}{T_{diesel}} & -\frac{1}{T_{diesel}s_{diesel}} \\ \frac{I_{s_e}}{2H} & \frac{V_{sc_e} - 2R_s I_{s_e}}{2H} & 0 & 0 & 0 & \frac{1}{2H} & \frac{-D}{2H} \end{bmatrix}$$

$$B_1 = \begin{bmatrix} 0 & 0 & 0 \\ -\frac{V_{dc_e}}{L_c} & 0 & 0 \\ \frac{I_{s_e}}{C_{dc}} & -\frac{I_{sd_e}}{C_{dc}} & -\frac{I_{sq_e}}{C_{dc}} \\ 0 & \frac{V_{dc_e}}{L_f} & 0 \\ 0 & 0 & \frac{V_{dc_e}}{L_f} \\ 0 & 0 & 0 \\ 0 & 0 & 0 \end{bmatrix} \quad B_2 = \begin{bmatrix} 0 \\ 0 \\ 0 \\ 0 \\ 0 \\ 0 \\ -\frac{1}{2H} \end{bmatrix}$$

$$C = [0 \quad 0 \quad 0 \quad 0 \quad 0 \quad 0 \quad 1]$$

$$D_1 = [0 \quad 0 \quad 0]$$

$$D_2 = [0]$$

Fig.7. State-space model matrices of robust control system.

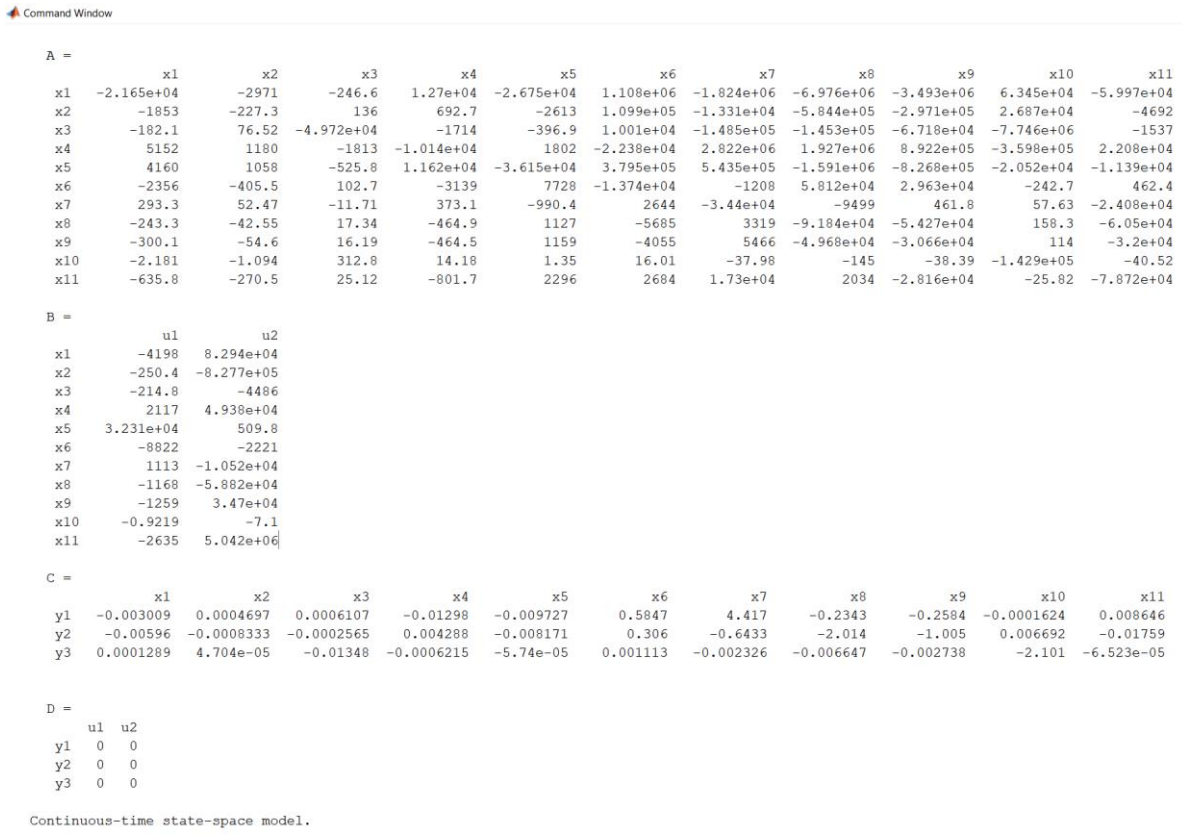

Command Window

A =

	x1	x2	x3	x4	x5	x6	x7	x8	x9	x10	x11
x1	-2.165e+04	-2971	-246.6	1.27e+04	-2.675e+04	1.108e+06	-1.824e+06	-6.976e+06	-3.493e+06	6.345e+04	-5.997e+04
x2	-1853	-227.3	136	692.7	-2613	1.099e+05	-1.331e+04	-5.844e+05	-2.971e+05	2.687e+04	-4692
x3	-182.1	76.52	-4.972e+04	-1714	-396.9	1.001e+04	-1.485e+05	-1.453e+05	-6.718e+04	-7.746e+06	-1537
x4	5152	1180	-1813	-1.014e+04	1802	-2.238e+04	2.822e+06	1.927e+06	8.922e+05	-3.598e+05	2.208e+04
x5	4160	1058	-525.8	1.162e+04	-3.615e+04	3.795e+05	5.435e+05	-1.591e+06	-8.268e+05	-2.052e+04	-1.139e+04
x6	-2356	-405.5	102.7	-3139	7728	-1.374e+04	-1208	5.812e+04	2.963e+04	-242.7	462.4
x7	293.3	52.47	-11.71	373.1	-990.4	2644	-3.44e+04	-9499	461.8	57.63	-2.408e+04
x8	-243.3	-42.55	17.34	-464.9	1127	-5685	3319	-9.184e+04	-5.427e+04	158.3	-6.05e+04
x9	-300.1	-54.6	16.19	-464.5	1159	-4055	5466	-4.968e+04	-3.066e+04	114	-3.2e+04
x10	-2.181	-1.094	312.8	14.18	1.35	16.01	-37.98	-145	-38.39	-1.429e+05	-40.52
x11	-635.8	-270.5	25.12	-801.7	2296	2684	1.73e+04	2034	-2.816e+04	-25.82	-7.872e+04

B =

	u1	u2
x1	-4198	8.294e+04
x2	-250.4	-8.277e+05
x3	-214.8	-4486
x4	2117	4.938e+04
x5	3.231e+04	509.8
x6	-8822	-2221
x7	1113	-1.052e+04
x8	-1168	-5.882e+04
x9	-1259	3.47e+04
x10	-0.9219	-7.1
x11	-2635	5.042e+06

C =

	x1	x2	x3	x4	x5	x6	x7	x8	x9	x10	x11
y1	-0.003009	0.0004697	0.0006107	-0.01298	-0.009727	0.5847	4.417	-0.2343	-0.2584	-0.0001624	0.008646
y2	-0.00596	-0.0008333	-0.0002565	0.004288	-0.008171	0.306	-0.6433	-2.014	-1.005	0.006692	-0.01759
y3	0.0001289	4.704e-05	-0.01348	-0.0006215	-5.74e-05	0.001113	-0.002326	-0.006647	-0.002738	-2.101	-6.523e-05

D =

	u1	u2
y1	0	0
y2	0	0
y3	0	0

Continuous-time state-space model.

Fig.8. Computing H-infinity controller in Matlab software.

4.2 Selecting weighting functions

Based on (4) and ω_B^* is defined as 2, the weighting functions for the controller input signals (Δf) and the controller output signals (Δm_{sc}, Δm_d, Δm_q) are selected respectively as follows:

$$\Delta f: \quad W_v = \frac{0,5s+2}{s+0,02} \tag{13}$$

$$\Delta m_{sc}: \quad W_{u1} = \frac{0,5s+2}{s+0,1} \tag{14}$$

$$\Delta m_d: \quad W_{u2} = \frac{0,5s+2}{s+0,1} \tag{15}$$

$$\Delta m_q: \quad W_{u3} = \frac{0,5s+2}{s+0,1} \tag{16}$$

4.3 Computing H-infinity controller

To compute the H-infinity controller, we use *hinfsyn* command in Matlab software. The calculation result is the minimum value of $\gamma = \min_K \|N(K)\|_\infty$ The command is [K, CL, gamma] = *hinfsyn*(P, NMEAS, NCON, 'GMIN', 1) [19].

After many trials, $\gamma_{\min} = 1$ is selected (corresponding to

Table 1. Simulation Parameters of Studied System

Case	Unit power			
	Load	**PV system**	**Diesel generator**	**ESS**
Case 1	1,2 MW	Initial: 200 kW Maximum: 200kW	Initial: 1 MW	Initial: 0 W Maximum: infinity (assumed)
Case 2	1,2 MW	Initial: 400 kW Maximum: 400kW	Initial: 800 kW	Initial: 0 W Maximum: infinity (assumed)
Case 3	1,2 MW	Initial: 600 kW Maximum: 600kW	Initial: 600 kW	Initial: 0 W Maximum: infinity (assumed)

the 'GMIN',1 option in the *hinfsyn* command). Here the value $\gamma_{\min} = 1$ is used for simulation because it is small enough to give the optimal controller while ensuring the quality of the system. Then, the controller K can be determined in the Matlab software in Fig. 8.

5. SIMULATION RESULTS

The parameters of each unit in studied Microgrid model used for simulation process are assumed in Table I. Different penetration levels of PV system are considered in the simulation. Specifically, the PV power is increase from 200kW (Case 1) to 400kW (Case 2), then 600kW (Case 3) at last. The load power demand stays remain during the simulation. The maximum capacity of ESS is assumed to be infinity, that means it can response to any changes of PV power. For PV system, the input irradiance scenario is given in Fig. 9 (assumed that the input temperature is 25℃ all the time).

The perturb and observe (P&O) MPPT algorithm is applied to the PV system. Moreover, the previous research of droop controller in [6] is also considered to compare with the designed H-infinity controller.

In Fig. 9, solar irradiance drops to 100 W/m^2 at the 5th second and remains until the 11th second. Then, it rises again to 1000 W/m^2 from the 11th second to the 12th second. However, the P&O algorithm in the PV system cannot track the maximum power point during the rising of solar irradiance because of short rising time. As the result, the PV power does not reach the maximum at that time, as shown in Fig. 10.

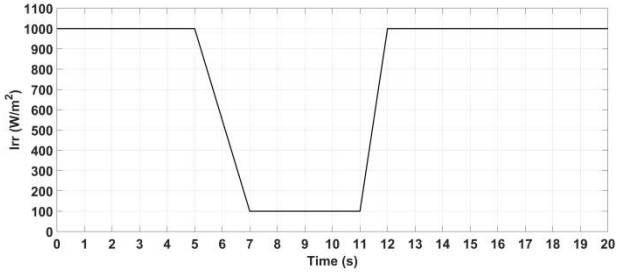

Fig. 9. Solar irradiance scenario.

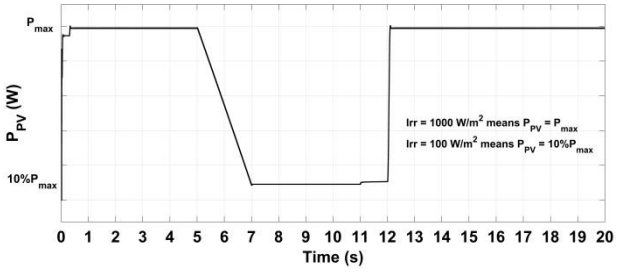

Fig. 10. Output PV power with corresponding solar irradiance.

The simulation results, including the frequency of the system and the response of DG units, for three different cases of PV penetration levels are shown from Fig. 11 to Fig. 16.

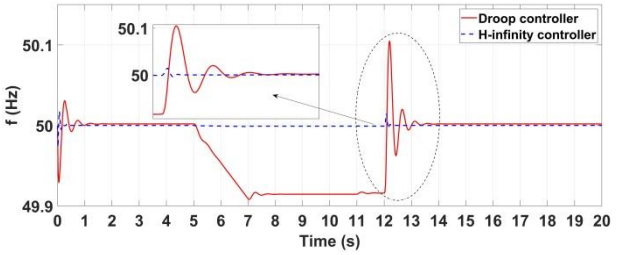

Fig. 11. Frequency of the system in Case 1.

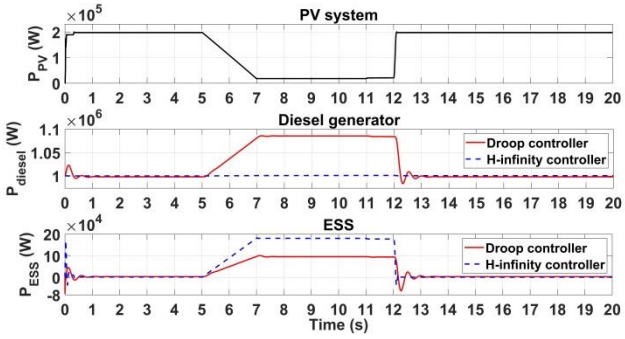

Fig. 12. Response of DG units in Case 1.

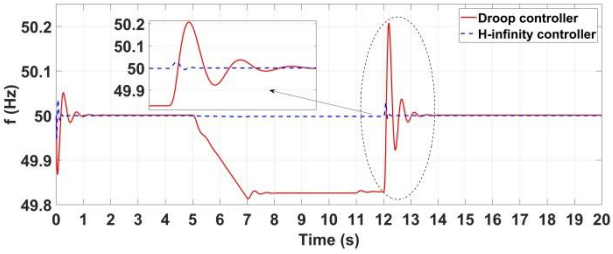

Fig.13. Frequency of the system in Case 2.

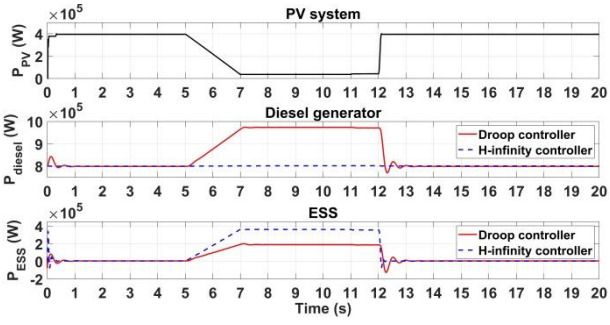

Fig. 14. Response of DG units in Case 2.

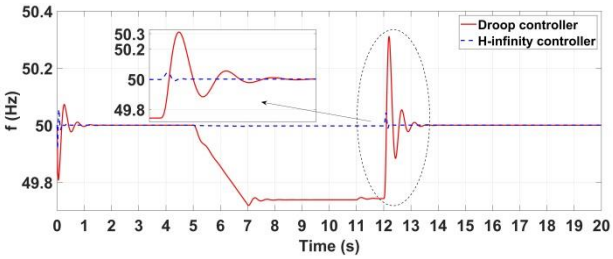

Fig.15. Frequency of the system in Case 3.

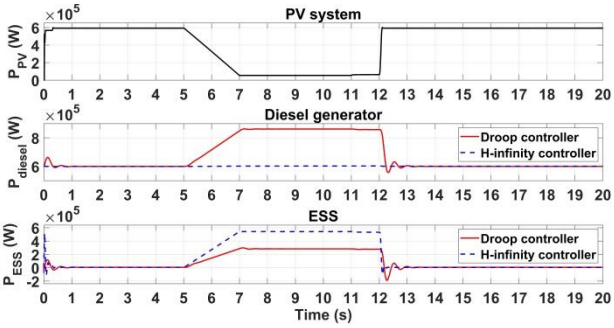

Fig. 16. Response of DG units in Case 3.

As can be seen from simulation results, with different cases of PV power, the frequency of the system shows better response when using the H-infinity controller. When the PV power changes suddenly and sharply, at the 12th second, the H-infinity controller responds quickly to the power fluctuation and keeps the frequency around the nominal value (50 Hz). With the droop controller, the system cannot bring the frequency back to its nominal value from the 5th second to the 12th second and the peak value of the frequency goes extremely high at about the 12th second. Especially, in Case 3, the frequency remains stable and the frequency fluctuation is not decent with H-infinity control. In contrast, the frequency fluctuation when using droop control is strongly aggressive, thus the frequency is out of the acceptable range (from 49.8 Hz to 50.2 Hz).

Moreover, from the results of DG units' response, there are differences in the power sharing between diesel generator and ESS. With the droop control, the power injected to the system is divided equally between both DG units. With the H-infinity controller, Microgrid only receives power from ESS while the diesel generator does not participate in the power sharing. This remarkable aspect will be considered in the calculation of DG units for an optimal and relevant control strategy when using robust H-infinity control method.

6. CONCLUSION

The theory of Microgrid and robust control was briefly and concisely presented in the paper. Robust H-infinity control method for Microgrid has been proposed and shown through figures and equations as well as simulation process using Matlab/Simulink software. The simulation results show that, when increasing the capacity of the renewable energy source, the system frequency will fluctuate and exceed the acceptable limit. Therefore, H-infinity controller was designed to solve that problem to expand the penetration of renewable energy into the system. Compared to traditional method (droop control), H-infinity controller shows remarkable performance in the frequency stability of the Microgrid. However, H-infinity controller is too complicated because of its high order, so it is not practical to make hardware application. In the future, authors will study to reduce the complexity of the H-infinity controller for practical application. In addition, other advanced algorithms will be considered to apply for islanded Microgrid control.

ACKNOWLEDGMENT

This work was supported by The University of Danang, University of Science and Technology, code number of Project: **T2020-02-07**.

REFERENCES

[1] N. Tan, L. Hong Lam, Q. Duong, N. Hieu, and K. Le, "A Thorough Overview of Hierarchical Structure of Microgrid Systems," 2018, pp. 710–715.

[2] F. Katiraei, R. Iravani, N. Hatziargyriou, and A. Dimeas, "Microgrids Management," *Power Energy Mag. IEEE*, vol. 6, pp. 54–65, 2008.

[3] M. Mahmoud, S. Hussain, and M. Abido, "Modeling and Control of Microgrid: An Overview," *J. Franklin Inst.*, vol. 351, 2014.

[4] F. Katiraei, R. Iravani, N. Hatziargyriou and A. Dimeas, "Microgrids management," in *IEEE Power and Energy Magazine*, vol. 6, no. 3, pp. 54-65, May-June 2008.

[5] J.-O. Lee, E.-S. Kim, and S.-I. Moon, "Determining P-Q Droop Coefficients of Renewable Generators for Voltage Regulation in an Islanded Microgrid," *Energy Procedia*, vol. 107, pp. 122–129, 2017.

[6] V. Nguyen, D. Hoang, H. Nguyen Huu, K. Le, T. Truong, and Q. Le, "Analysis of Uncertainties for the Operation and Stability of an Islanded Microgrid," 2019, pp. 178–183.

[7] E. Planas, A. Gil-de-Muro, J. Andreu, I. Kortabarria, and I. de Alegría, "General aspects, hierarchical controls and droop methods in microgrids: A review," *Renew. Sustain. Energy Rev.*, vol. 17, no. C, pp. 147–159, 2013.

[8] Q. L. Lam, A. Bratcu, and D. Riu, "Robustness Analysis of Primary Frequency H∞ Control in Stand-alone Microgrids with Storage Units," in *IFAC-PapersOnLine*, 2016, vol. 49, pp. 123–128.

[9] T. Kerdphol, F. Rahman, Y. Mitani, and M. Watanabe, "Robust Virtual Inertia Control of an Islanded Microgrid Considering High Penetration of Renewable Energy," *IEEE Access*, vol. 6, pp. 625–636, 2018.

[10] Y. Khayat, M. Naderi, Q. Shafiee, M. Fathi, and H. Bevrani, "Robust single primary control loop for AC microgrids," 2018, pp. 505–509.

[11] B. Sedhom, A. Hatata, M. El-Saadawi, and H. Abd-Rabo, "Robust Adaptive H-Infinity based Controller for Islanded Microgrid Supplying Non-Linear and Unbalanced Loads," *IET Smart Grid*, 2019.

[12] J. Zhao and C. Wang, "Frequency stability of microgrids based on H∞ methods," in *2016 35th Chinese Control Conference (CCC)*, 2016, pp. 10079–10084.
[13] B. Nguyen, V. Pham, V. Nguyen, D. Hoang, T. Truong, and H. Nguyen, "A New Maximum Power Point Tracking Algorithm for the Photovoltaic Power System," 2019, pp. 159–163.
[14] B. Nguyen, V. Nguyen, Q. Duong, K. Le, H. Nguyen Huu, and A. Doan, "Propose a MPPT Algorithm Based on Thevenin Equivalent Circuit for Improving Photovoltaic System Operation," *Front. Energy Res.*, vol. 8, 2020.
[15] Tan, Nguyen Van, et al. "A Proposal for an MPPT Algorithm Based on the Fluctuations of the PV Output Power, Output Voltage, and Control Duty Cycle for Improving the Performance of PV Systems in Microgrid." *Energies*, vol. 13, no. 17, 2020, p. 4326.
[16] P. Kundur, N. J. Balu, and M. G. Lauby, *Power system stability and control*, vol. 7. McGraw-hill New York, 1994.
[17] S. Skogestad and I. Postlethwaite, *Multivariable feedback control: analysis and design*, vol. 2. Wiley New York, 2007.
[18] S. Bacha, I. Munteanu, and A. I. Bratcu. *Power electronic converters modeling and control*. Springer, 2014.
[19] Compute H-infinity optimal controller - MATLAB *hinfsyn* [Online]. Available: https://www.mathworks.com/help/robust/ref/hinfsyn.html.